Computer Applications in Electrical Engineering
Vol. 14 *2016*
DOI 10.21008/j.1508-4248.2016.0021

Analysis of multiphase synchronous machines with fractional slot concentrated windings

Wojciech Szeląg, Cezary Jędryczka
Poznań University of Technology
60–965 Poznań, ul. Piotrowo 3A, e–mail: {wojciech.szelag;
cezary.jedryczka}@put.poznan.pl

The paper deals with analyses of multiphase fractional slot permanent magnet synchronous machines with concentrated windings. The advantages of studied machines have been discussed. Studied in the paper multiphase machines contain the number of phases in multiple of 3, facilitating the application of commonly used 3–phase intelligent power modules to build the multiphase supply system. The coding convention, an algorithm and software for synthesis and analysis of multiphase fractional slot concentrated windings have been developed. To verify presented algorithm the field approach has been employed. The professional FEM package Maxwell has been used to determine functional parameters of the test machine with different types of windings. Selected results of simulations of studied multiphase machines with different phase number and winding layouts have been presented and analyzed.

KEYWORDS: Permanent magnet synchronous machines, multiphase machines, fractional slot concentrated winding

1. Introduction

In the past few years, the permanent magnet synchronous machines with fractional slot concentrated windings have become the point of interest for many research and design teams [1, 2, 4, 5, 7]. The key advantages of these machines include lower cost windings design, shorter end turns, lower winding resistance all contributing to the increase of performance and efficiency [1, 3, 4] in relation to the classical AC machines with distributed windings. The advantages of fractional slot concentrated winding (FSCW) machines are especially apparent for low speed applications such as direct drive torque motors, elevator industry, wind turbine generators and marine propulsions systems [3, 4, 5]. However, these machines suffer from relatively high torque ripple, stray losses and magnetic noise due to the presence of sub and super harmonics in the magnetomotive force (*mmf*) spatial distribution [1, 2]. To mitigate these problems, several researchers proposed utilization of sources with a number of phases greater than 3. Based on published results and our own experience, these multiphase machines offer many advantages, including: low torque ripple, high winding factor and high efficiency [1, 3, 5]. On the other hand, powering and controlling machines with 5, 7 or 10 phases require development of customized inverters and novel control strategies. To reduce inverter costs, the multiphase machines discussed here contain the number of phases in multiple of 3, facilitating the application of commonly used 3–phase intelligent power modules. In other words, multiphase machines described herein may be powered by a given number of 3–phase commercially available drives/inverters. While these drives must be synchronized with proper shift angle between the 3–phase stars of currents, the galvanic connection between drives is not necessary. Using such multi–drive power supply system offers the following advantages: increased robustness, fault tolerance and flexibility in meeting requested machine performance. For example, if the requested machine output power is above the capability of the existing 3–phase drive, it may be supplied from two, three or four already developed drives rather than building a new, higher power drive. Obviously, the multi–drive supply system offers additional capability to supply the 3–phase machines with split up windings. Due to the presence of mutual inductances between phases, however, such machines are less fault tolerant than multiphase machines considered herein. Two examples of using a multi–drive supply system to power real 6–phase and dual 3–phase permanent magnet synchronous machine (PMSM) have been illustrated schematically in Fig. 1

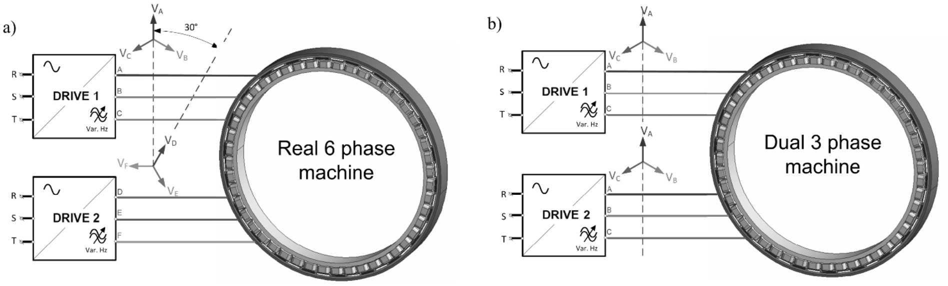

Fig. 1. Illustration of multi–drive supply system for: a) real 6–phase; and b) dual 3–phase PMSM

2. Multiphase fractional slot machines with concentrated windings

The theory dealing with the multiphase fractional slot concentrated windings machines is in the early phase of development. There lack of complex approaches and algorithms allowing for design of magnetic circuits of such machines in respect of defined requirements. In the conducted researches the number of stator slots, rotor poles and structure of the winding are sought to: achieve low torque ripples, minimize sub and super harmonics content in the magnetomotive force distribution as well as maximize winding factor or balancing the distribution of normal forces acting on the stator. Nevertheless publications in this field focus mainly on analysis of chosen aspects of the multiphase machines with given number of poles and slots [5, 7]. In other words there is lack of approaches allowing for optimal selection (for given requirements) of number of slots, rotor poles, arrangement of the magnet and structure of the winding of the multiphase permanent magnet synchronous machines with fractional slot concentrated windings.

Therefore in the paper the method of synthesis and analysis of fractional slot concentrated winding has been proposed. The algorithm and computer code for modeling and analysis of the windings of multiphase machines have been developed based on the circuit approach. This software has been used for the synthesis of the winding arrangements, calculation of winding factor and harmonic content of the magnetomotive force spatial distributions. These parameters have been used as figures of merit at the first stage of comparative analysis of different winding structures. In the second stage the field model of test PMSM with selected winding layouts have been developed using scripting language implemented in professional FEM package Maxwell. On the basis of determined magnetic flux distributions and calculated integral parameters of test machine selected functional parameters have been analyzed in the final stage comparison of machines of different number of phases and different winding structures.

Three basic structures of FSCW are illustrated in Fig. 2 [1, 4, 8]. Two types of double layer and one type with single layer windings are generally known. In the case of two layer windings, the coils are wounded as shown in Fig. 2a.

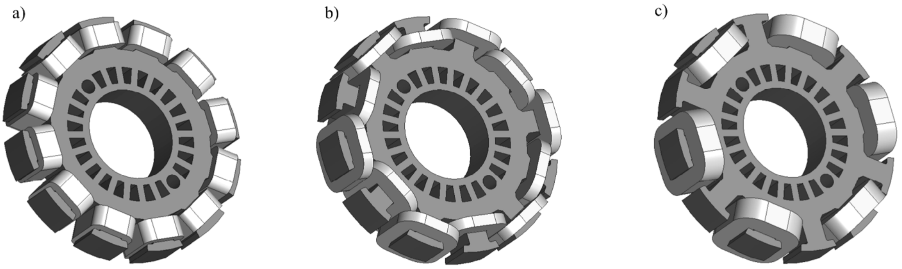

Fig. 2. Illustration of FSCW with a), b) two layers (all teeth wound) and c) single layer (alternative teeth wound) windings

This is in contrast to the classical manner known from the AC machines with distributed windings shown for comparison in Fig. 2b. In FSCW machines with single layer windings, each slot consists of only one coil's side as shown in Fig. 2c. Consequently, every second teeth remains unwounded. As such, terminology including "all teeth wound" and "alternative teeth wound" windings can be found in the literature as synonyms for single and double layer windings.

In this paper, the classical naming convention, i.e. single and double layer winding has been used instead.

3. Winding pattern determination algorithm

Several methods have been developed to determine winding patterns for 3–phase FSCW machines [4, 6]. These are based on phasor diagrams and numbers of poles [4, 2, 8]. One of the most comprehensive methodologies has been described in [4]. First, to determine the winding magnetomotive force waveform, the method of coding the arrangement of coils over the slots of the machine is needed. For FSCW machines, the commonly used approach is based on the letter notation *ABC* and *A'B'C'* for positive and negative coil sides placed in slots of the phases *A*, *B* and *C*, respectively.

For example the simplest 3–phase double layer winding pattern (for number of slots per pole per phase q equal to 1/2 and 1/4) may be written out as *...A|A' B|B' C|C'...* (here, the symbols "|" have been used to mark the armature core teeth). This pattern corresponds to two or four magnetic poles within the machine rotor and is repeated along the circumference of the stator n times (where n is an integer) according to the number of coils per phase of the machine. Such pattern is treated as the fundamental winding pattern (FWP) and facilitates splitting the machine windings – for connecting the coils into parallel branches.

There exist several different fundamental winding patterns for the 3–phase machines defined for a given number of q slots per pole, per phase [6, 8]. Employing letter notation discussed above for the coding of the multiphase machines results in complex algorithms of FWP synthesis. Thus, a simpler method based on numbering the phasors has been proposed. The considered multiphase systems can be defined by the shift angle β:

$$\beta = \frac{\pi}{m} \tag{1}$$

and by parameter k describing the number of 3–phase subsystems, where m is the number of phases and $k = m/3$.

Examples of thus formed phasor systems, such as voltage supply for the 3, 6 and 9 of the phase shown in Fig. 3. The shift angle describes the phase offset between a) the successive phasors of a multiphase system and b) three phase subsystems as shown in phasor diagrams in Fig. 3. These shifted 3–phase subsystems constitute the multiphase voltage system defined as follows:

$$u_{i,j} = U_m \sin\left[\omega t - (j-1)\frac{2}{3}\pi - (i-1)\beta\right] \tag{2}$$

where $i = 1...k$, $j = 1, 2, 3$.

Two methodologies for the synthesis of multi–star multiphase FSCW have been proposed and tested. In the first, simpler methodology, the winding layout is searched for desired number of phases and slots of the machine basing only on the *mmf* space distribution analysis, while in the second method, more complex one, the desired number of poles is included for consideration. In both methods the same convention of coding the winding layout is applied.

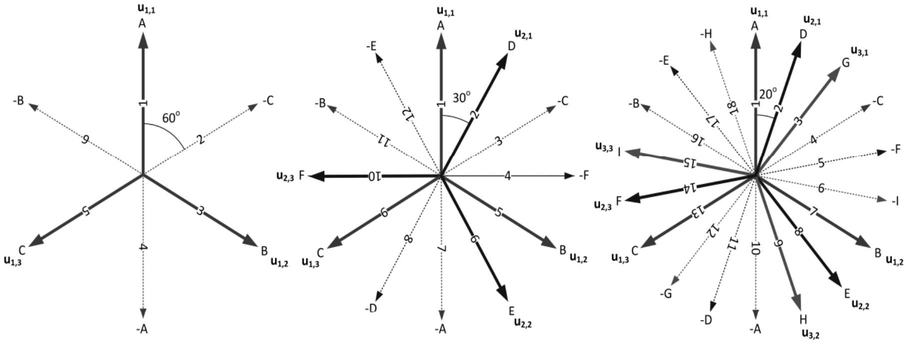

Fig. 3. Phasor diagrams of systems with: a) $m = 3$, $\beta = 60°$ and number of stars $k = 1$; b) $m = 6$, $\beta = 30°$ and $k = 2$; c) $m = 9$, $\beta = 20°$ and $k = 3$

The phasors in the considered system are described by numbers from 1 to $2m$ – see the examples of the phasor diagrams of the 3–, 6– and 9–phase systems shown in Fig. 3. By introducing the numeration of phasors as shown in Fig. 3, the fundamental winding patterns can be coded out as a set of numbers. Such an approach significantly simplifies the algorithm of synthesis of the multiphase winding arrangements. For example, FWP discussed above, consisting of 3–phase machines with q equal to 1/2 or 1/4, can be written out as: *...1|4 3|6 5|2....* For real 6–phase and 9–phase machines, the FWP can be determined to the first harmonic of the magnetic field introduced by rotor magnets by searching the phasors with the smallest phase shift angle between slot *mmf* and induced *emf.* Using this approach, FWP for 6– and 9–phase machines using the introduced phasor number notation can be defined as *...1|7 6|12 11|5 4|10 9|3 2|8 7|1 12|6 5|11 10|4 3|9 8|2...* and *1|10 9|18 17|8 7|16 15|6 5|14 13|4 3|12 11|2...,* respectively. The demonstrated numeric notation can be easily translated into the letter representation. Naming the phases of the first 3–phase system as *ABC*, second as *DEF* and third as *GHI*, the simplest winding patterns can be expressed as *..A|A' B|B' C|C'...* for the 3–phase machine, *...A|A' E|E' B'|B F'|F C|C' D|D' A'|A E'|E B|B' F|F' C'|C D'|D...* for the 6–phase machine and *...A|A' H|H' E'|E B|B' I|I' F'|F C|C' G|G' D'|D...* for the nine phase machine.

To determine multiphase winding patterns, a custom computer code suited for the analysis and synthesis of *mmf* distribution in the FSCW machines was developed. The exemplary designed winding templates for 3– and 6–phase machines are shown in Fig. 4.

The methodology discussed above has been incorporated into coding convention, whereby the analytical approach of superimposing slot magnetomotive forces was combined with the Fast Fourier Transform (FFT) algorithm. In addition to determining winding patterns and FFT analysis of *mmf* waveforms, the developed software also facilitates calculation of the winding factor.

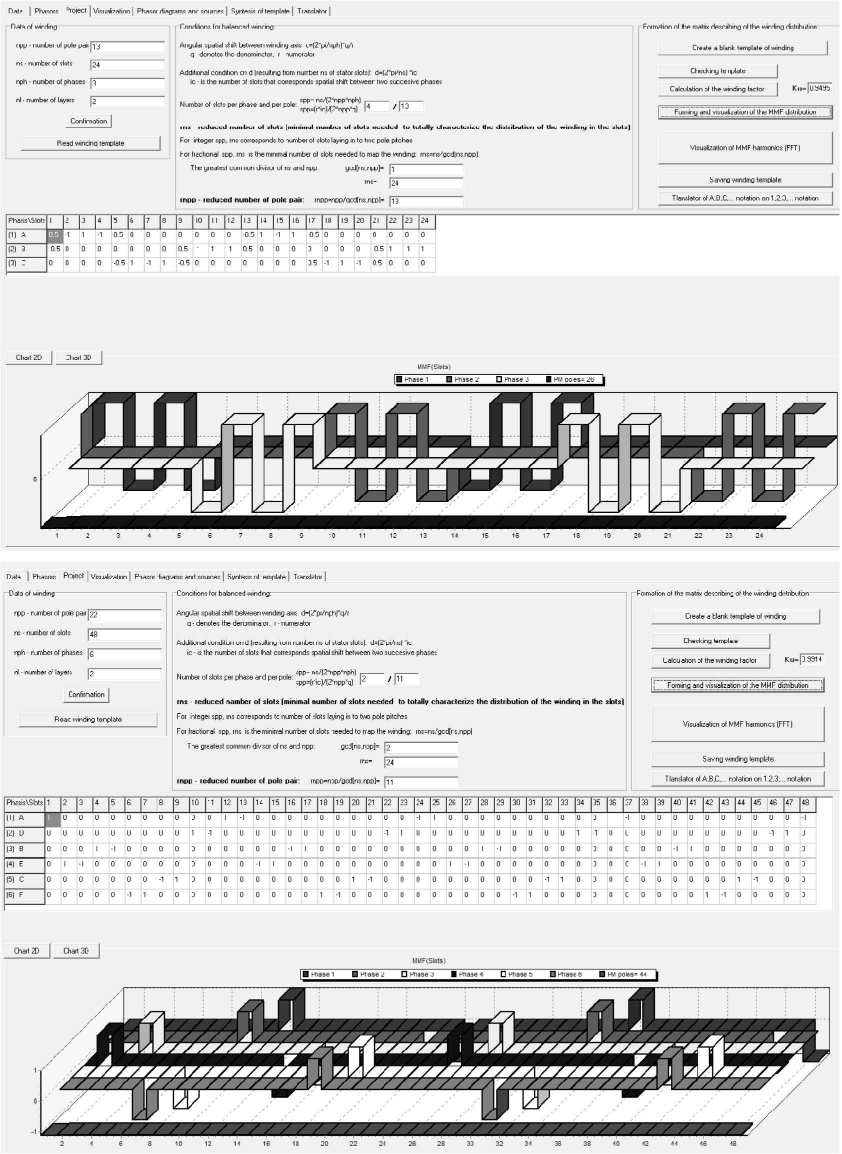

Data of winding

npp - number of pole pair: 13
ns - number of slots: 24
nph - number of phases: 3
nl - number of layers: 2

Conditions for balanced winding

Angular spatial shift between winding axis d=(2*pi/nph)*q/r
q - denotes the denominator, r - numerator

Additional condition on d (resulting from number ns of stator slots): d=(2*pi/ns)*ic
ic - is the number of slots that corresponds spatial shift between two succesive phases

Number of slots per phase and per pole: spp= ns/(2*npp*nph) spp=(r*ic)/(2*npp*q) 4 / 13

rns - reduced number of slots (minimal number of slots needed to totally characterize the distribution of the winding in the slots)

For integer spp, rns corresponds to number of slots laying in to two pole pitches

For fractional spp, rns is the minimal number of slots needed to map the winding: rns=ns/gcd[ns,npp]

The greatest common divisor of ns and npp: gcd[ns,npp]= 1
rns= 24

rnpp - reduced number of pole pair: rnpp=npp/gcd[ns,npp]= 13

Formation of the matrix describing of the winding distribution

Ku= 0.9495

Phasis\Slots	1	2	3	4	5	6	7	8	9	10	11	12	13	14	15	16	17	18	19	20	21	22	23	24
(1) A	0.5	-1	1	-1	0.5	0	0	0	0	0	0	0	-0.5	1	-1	1	-0.5	0	0	0	0	0	0	0
(2) B	0.5	0	0	0	0	0	0	0	0.5	1	1	1	0.5	0	0	0	0	0	0	0	0.5	1	1	1
(3) C	0	0	0	0	-0.5	1	-1	1	-0.5	0	0	0	0	0	0	0	0.5	-1	1	-1	0.5	0	0	0

Data of winding

npp - number of pole pair: 22
ns - number of slots: 48
nph - number of phases: 6
nl - number of layers: 2

Conditions for balanced winding:

Angular spatial shift between winding axis d=(2*pi/nph)*q/r
q - denotes the denominator, r - numerator

Additional condition on d (resulting from number ns of stator slots): d=(2*pi/ns)*ic
ic - is the number of slots that corresponds spatial shift between two succesive phases

Number of slots per phase and per pole: spp= ns/(2*npp*nph) spp=(r*ic)/(2*npp*q) 2 / 11

rns - reduced namber of slots (minimal number of slots needed to totally characterize the distribution of the winding in the slots)

For integer spp, rns corresponds to number of slots laying in to two pole pitches

For fractional spp, rns is the minimal number of slots needed to map the winding: rns=ns/gcd[ns,npp]

The greatest common divisor of ns and npp: gcd[ns,npp]= 2
rns= 24

rnpp - reduced number of pole pair: rnpp=npp/gcd[ns,npp]= 11

Formation of the matrix describing of the winding distribution

Ku= 0.9914

Phasis\Slots	1	2	3	4	5	6	7	8	9	10	11	12	13	14	15	16	17	18	19	20	21	22	23	24
(1) A	1	0	0	0	0	0	0	0	0	0	0	1	-1	0	0	0	0	0	0	0	0	0	0	-1
(2) D	0	0	0	0	0	0	0	0	0	1	-1	0	0	0	0	0	0	0	0	0	0	-1	1	0
(3) B	0	0	0	1	-1	0	0	0	0	0	0	0	0	0	0	-1	1	0	0	0	0	0	0	0
(4) E	0	1	-1	0	0	0	0	0	0	0	0	0	0	-1	1	0	0	0	0	0	0	0	0	0
(5) C	0	0	0	0	0	0	0	-1	1	0	0	0	0	0	0	0	0	0	0	1	-1	0	0	0
(6) F	0	0	0	0	0	-1	1	0	0	0	0	0	0	0	0	0	0	1	-1	0	0	0	0	0

Phasis\Slots	25	26	27	28	29	30	31	32	33	34	35	36	37	38	39	40	41	42	43	44	45	46	47	48
(1) A	1	0	0	0	0	0	0	0	0	0	0		-1	0	0	0	0	0	0	0	0	0	0	-1
(2) D	0	0	0	0	0	0	0	0	0	1	-1	0	0	0	0	0	0	0	0	0	0	-1	1	0
(3) B	0	0	0	1	-1	0	0	0	0	0	0	0	0	0	0	-1	1	0	0	0	0	0	0	0
(4) E	0	1	-1	0	0	0	0	0	0	0	0	0	0	-1	1	0	0	0	0	0	0	0	0	0
(5) C	0	0	0	0	0	0	0	-1	1	0	0	0	0	0	0	0	0	0	0	1	-1	0	0	0
(6) F	0	0	0	0	0	-1	1	0	0	0	0	0	0	0	0	0	0	1	-1	0	0	0	0	0

Fig. 4. Developed software for the analysis and synthesis of winding template for multiphase fractional slot permanent magnet synchronous machines: a) winding template for 3–phase (on top) and b) for 6–phase machines (bottom)

In particular, the fundamental winding factor, k_{wf}, has been calculated as the ratio of *mmf* waveform fundamental harmonic amplitude to the slot *mmf* amplitude. For verification purposes, the classical approach of determining the winding factor based on number of poles has also been implemented. The adopted method is based on the summation of the electromotive forces (*emfs*) induced in the coil sides forming the phase winding (i.e., over the slots of the machine). When calculating the fundamental winding factor, it has been assumed that *emfs* are induced by the fundamental harmonic of the magnetic field distribution excited by permanent magnet of the machine. Accordingly, the k_{wf} can be expressed as:

$$k_{wf} = \left| \sum_{i=1}^{n_s} W_j[i] \vec{E}_i \right| / n_b \tag{3}$$

where $\vec{E}_i = e^{j2p\pi i/n_s}$ is the unit vector defining the direction of *emf* induced in the coil side located in the i–th slot, p is the number of pole pairs, n_s is the number of slots in the stator, n_b is the number of coil sides forming the j–th phase winding, matrix $W_j[i]$ consist of n_s elements and defines assignment of the coil side in i–th slot to the j–th phase. Specifically, if the coil side in i–th slot does not belong to the j–th phase the $W_j[i] = 0$. Otherwise, $W_j[i]$ is equal to 1 or −1 according to current flow direction. For the double layer windings the elements of $W_j[i]$ equals to 0, 0.5 and −0.5, respectively.

In addition to winding factor and sub–harmonic analysis used to assess winding layouts, the developed software also calculates figures of merit including: last common multiply (*LCM*) and greatest common divisor (*GCD*) between poles and slot numbers.

Discussed above methodology has been applied to 3–, 6– and 9– phases machines discussed earlier. Their fundamental winding factors k_{wf} were determined to be 0.866, 0.966 and 0.985, respectively. Achieving higher winding factors with an increasing number of phases is attributed to better fitting of the fundamental magnetic field distribution introduced by permanent magnets due to higher number of available different phasors along the pole pitch of the machine.

4. Analysis of mmf distribution in test machine

The comparative analysis of the *mmf* waveforms between the 3–phase and 6–phase test machines has been performed. To avoid the influence of the latest common multiply (LCM) and the greatest common divider (GCD) between the number of poles and slots, the 6–phase and 3–phase windings of the test machine with 48 slots and 44 poles have been determined. Single as well as double layer windings for the 3– and 6–phase machines have been examined. The studied winding layouts have been listed in Table 1.

Table 1. The studied winding layouts of the test machine

Notation	Description
3ph–SL	3–phase machine, single layer winding
3ph–DL	3–phase machine, double layer winding
6ph–SL	6–phase machine, single layer winding
6ph–DL	6–phase machine, double layer winding

The results of the performed *mmf* analysis have been reported in Table 2, summarizing the total harmonic distortion of *mmf* space distribution (*mmf* THD), fundamental winding factor (k_{wf}), percentage value (V_{ho}) of the highest sub–harmonic of *mmf* waveform and its order (O_{ho}).

Table 2. Summary of *mmf* waveform analysis of the considered windings (48 slot/44 pole machine)

Winding/machine	k_{wf}	V_{ho} [%]	O_{ho}	*mmf* THD [%]
3ph–SL	0.958	21.44	14	30.06
3ph–DL	0.949	17.15	14	19.99
6ph–SL	0.991	13.17	2	13.17
6ph–DL	0.983	1.73	2	1.73

The values of *mmf* in the slots for chosen time instants of the considered supply systems and subharmonic content in *mmf* distributions have been shown in Fig. 5a and Fig 5b respectively. It can be noted that for all studied windings the fundamental harmonic of the *mmf* is equal to 22 that correspond to 44 magnetic poles.

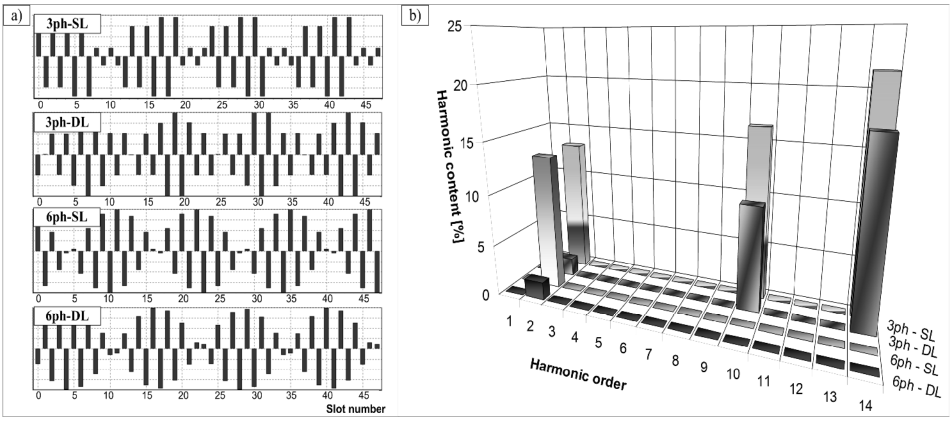

Fig. 5. Space distributions of *mmf* for chosen time snap shots a) and comparison of harmonic content in *mmf* b) for considered winding layouts

Obtained results confirm that increasing the number of phases lead out to increase of fundamental winding factor. Moreover for both single and double layer 6–phase windings the significant reduction of the subharmonic content of *mmf* waveform can be observed. Comparing the winding factor of single and double layer winding machines, it can be seen that a higher value of k_{wf} is obtained for single layer windings. However, it can be noticed that single layer windings introduces a second harmonic to the *mmf* distribution (~13% for both 3– and 6–phase winding cases).

5. Motor performance comparison

High values of winding factor suggest better fitting of the stator winding to the magnetic field excited by the permanent magnets placed in the rotor of the machine and thus better utilization of the magnetic circuit. To validate this thesis the finite element analysis of the test machines have been performed. The field model have been developed in the professional FEM package Maxwell EM. The four winding layouts of the PMSM test machine with 44 poles and 48 slots, studied in the previous section, have been implemented in 4 different 2D FEM models. As illustrated in Fig. 6, three different rotor structures have been considered. These included: a) a spoke type permanent magnet (SIPM), b) a surface permanent magnet (SPM) and c) an interior permanent magnet (IPM). The overall dimensions and stator slot shape have been kept the same across the studied winding layouts and rotor geometries. The mass of the permanent magnets has been kept the same for all three studied rotor structures. Similarly, the number of conductors per slot for single and double layer winding was kept the same. For the synthesis of the test machines windings the approach and software described in section 2 have been utilized.

Machine major data:

Outer diamater : *320mm*

Number of slots: *48*

Number of poles: *44*

Stack lenght: *55mm*

Magnets: *N42SH*

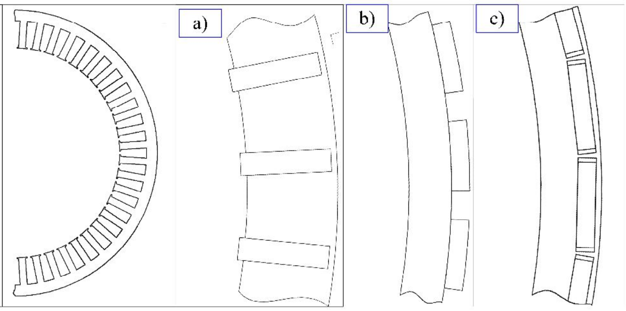

Fig. 6. Stator and the considered rotor structures of studied PMSM machine with 44 poles and 48 slots, a) SIPM; b) SPM and c) IPM

The exemplary magnetic field distributions in the SPM machines with 3– and 6–phase double layer windings are shown in Fig. 7 and Fig. 8, respectively.

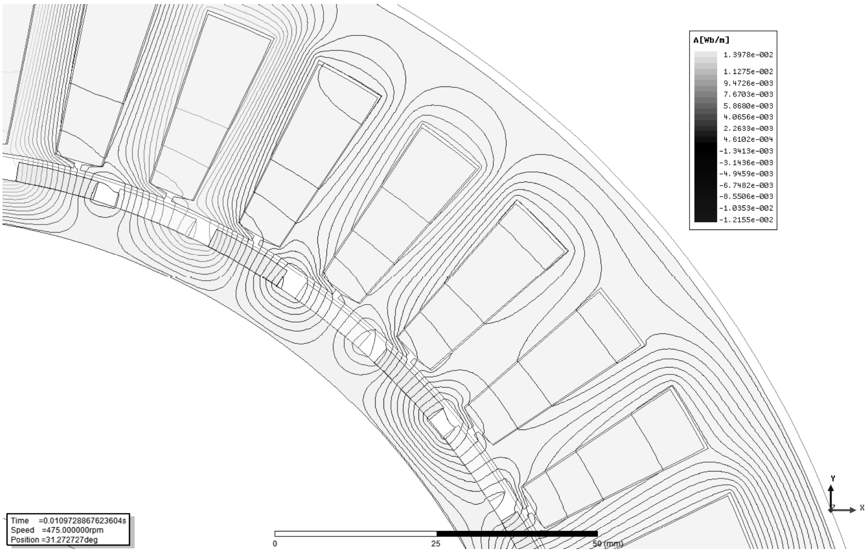

Fig. 7. Distribution of the magnetic field in the machines with SPM and 3–phase double layer winding at the rated current

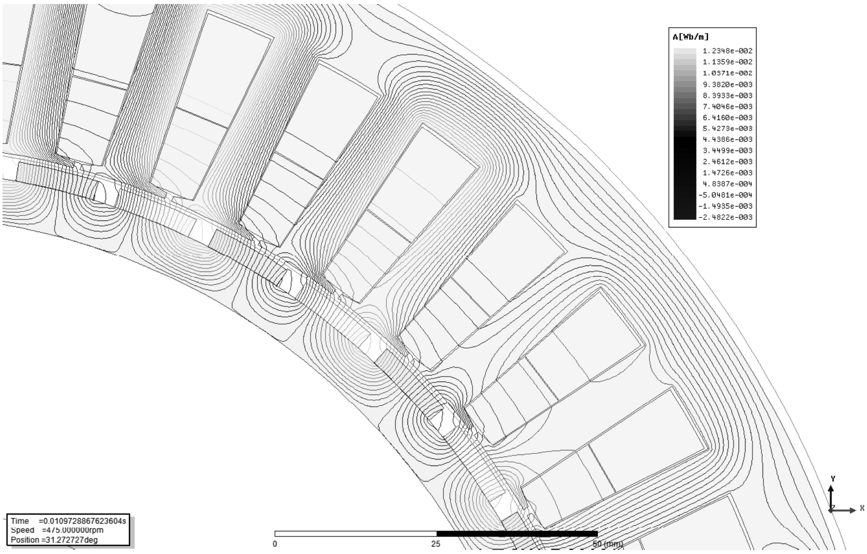

Fig. 8. Distribution of the magnetic field in the machines with SPM and 6–phase double layer winding at the rated current

The conducted studies have been focused on comparison of electromotive force (back *emf*) induced at no load state and electromagnetic torque value as wells as torque ripple analysis. The exemplary waveforms of the induced at open circuit line to line back *emf* of 3–phase double layer and 6–phase single layer winding machines have been shown in Figures 9b i 9d, respectively. In order to compare the level of back *emf* distortion discussed waveforms have been analyzed using FFT and obtained results have been shown in Fig. 7a i 7c, respectively.

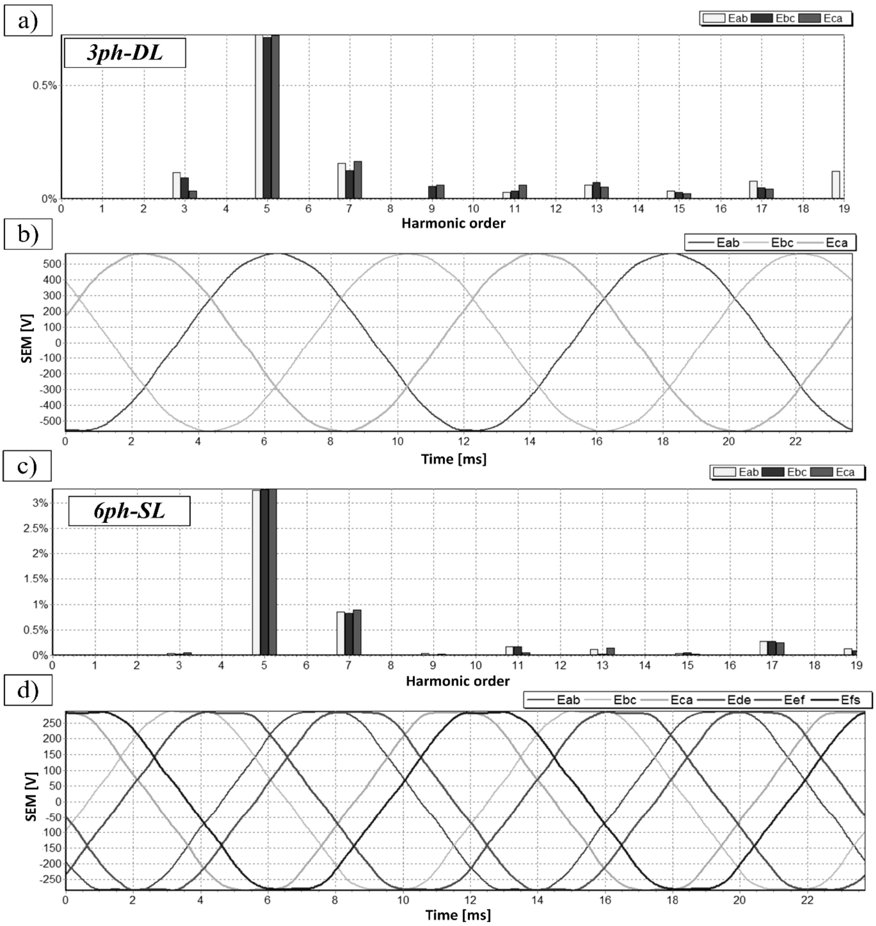

Fig. 9. Line to line back *emf* waveforms at open circuit and its percentage harmonic content for machine with 3–phase double layer winding a), b) and machine with 6–phase single layer winding c), d)

The harmonic contents of the discussed back *emf* waveforms have been compared in Fig. 10. It can be seen that considered machines with 6–phase windings characterize with higher level of distortion of the back *emf* waveforms. Especially increase of 5 and 7 harmonic can be observed. The higher level of back *emf* distortion for 6–phase is expectable due to reduced number of coils connected in series that are forming the phase *emf* in comparison to the studied machine with 3–phase.

The electromagnetic torque waveforms calculated for rated phase current equal to 50A (*rms* value) and torque angle α equal to α_m have been compared in Fig. 11a. The torque angle has been defined as a torque between rotor and stator field axes, while α_m is iteratively calculated value of the torque angle giving highest average value of the torque waveform at given *rms* value of supply current. For needs of quantitative assessment of the waveforms presented in Fig. 11a the average values T_{av} and torque ripple factors ε_T have been calculated and presented in Fig. 11b.

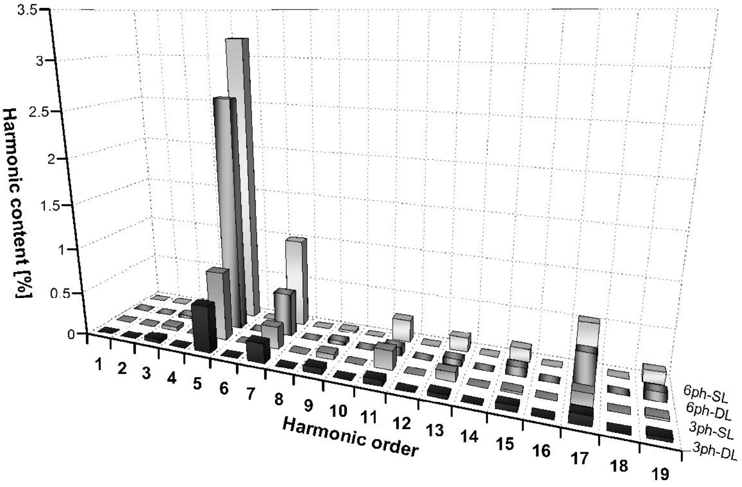

Fig. 10. Comparison of the percentage harmonic content in the line to line back *emf* waveforms at no load conditions

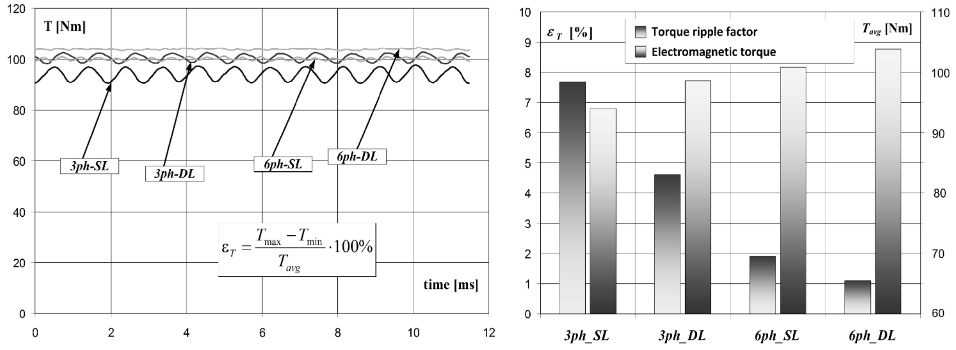

Fig. 11. Comparison of : a) electromagnetic torque waveforms and b) average value and torque ripples factors for considered windings

Studying the results the significant reduction of the torque ripples can be observed for machines with 6–phase windings in relation to their 3–phase counterparts. The value of the torque ripple factor ε_T for the worst variant is above 7%, while machine with 6–phase double layer winding characterize with torque ripples about 1%. Also, the increase of the average value of the electromagnetic torque waveform at given phase current can be noted for 6–phase machines. Wherein it is important to notice that the effective torque is higher for the both double layer, 3– and 6–phase windings in spite of the lower values of the fundamental winding factor calculated in section 3.

6. Conclusions

Analysing the presented results, it can be concluded that the considered 6–phase winding layouts are characterized by a lower content of sub–harmonics in the *mmf* waveform as compared with the 3–phase machines. The studied 6–phase machines also exhibited a higher average value of electromagnetic torque as compared to the referred 3–phase machines. Moreover, the investigated 6–phase PMSM machines with FSCW are characterized by significantly lower torque ripples.

According to findings presented in [2] presence of sub and super harmonics in magnetomotive force spatial distribution is the main source of increased eddy current losses in the machines with FSCW. Demonstrated, on the studied case problem example, reduction of the subharmonics of *mmf* for multiphase winding layouts should lead to reduction of power losses that together with reported better utilization of the magnetic circuit allow for design of high efficiency permanent magnet synchronous machines. Authors, currently are conducting an intensive researches aimed to confirm discussed above thesis. The results will be reported in further going publications.

In summary, machines with the proposed 6–phase windings offer improved functionality in relation to machines with the classic 3–phase FSCW. Besides the increase of the torque density, the 6–phase machines exhibit significantly lower torque ripples and reduced values of low order spatial harmonics in comparison to the studied 3–phase machines. The utilization of multi–drive supply systems allows for the further reduction of application costs for such machines, while simultaneously increasing their fault tolerance.

References

[1] El–Refaie A.M., Fractional–Slot Concentrated–Windings Synchronous Permanent Magnet Machines: Opportunities and Challenges, IEEE Transactions on Industrial Electronics, Vol. 57, No. 1, January 2010.

[2] Magnussen F, Lendenmann H., Member, Parasitic Effects in PM Machines With Concentrated Windings, IEEE Transactions on Industriary Applications, Vol. 43, No. 5, 2007.
[3] Piech J., Permanent Magnet Machines for Elevators in Super High–Rise Buildings, Council on Tall Buildings and Urban Habitat CTBUH 2014, pp. 823.
[4] Salminen P. Fractional slot permanent magnet synchronous motors for low speed applications, Acta Universitatis Lappeenrantaensis, 2004.
[5] Scuiller F., Charpentier J., Semail E., Multi–star multi–phase winding for a high power naval propulsion machine with low ripple torques and high fault tolerant ability, Vehicle Power and Propulsion Conference (VPPC), 2010, IEEE.
[6] Libert F., J. Soulard J. , Investigation on Pole–Slot Combinations for Permanent–Magnet Machines with Concentrated Windings, in Proc. ICEM, pp. 1–6, 2004.
[7] Valavi M., Nysveen A., Nilssen R., Robert D. Lorenz R.D., Rølvåg T., Influence of Pole and Slot Combinations on Magnetic Forces and Vibration in Low–Speed PM Wind Generators, IEEE Transaction on Magnetics, Vol. 50, No. 5, May 2014.
[8] Yang J., Liu G., Zhao W., Chen Q., Jiang Y., Sun L., et al., Quantitative comparison for fractional–slot concentrated–winding configurations of permanent magnet vernier machines, IEEE Transaction on Magnetics, Vol. 49, No. 7, July 2013.

(Received: 18. 11. 2016, revised: 25. 11. 2016)